Desorption of Arsenic Species during the Surfactant Enhanced Growth of Ge on Si(100)

Cindy L. Berrie[†] and Stephen R. Leone*[,‡]

JILA, National Institute of Standards and Technology and University of Colorado, and Department of Chemistry and Biochemistry, University of Colorado, Boulder, Colorado 80309-0440

Received: June 25, 2001; In Final Form: March 5, 2002

The desorption and scattering of As_4 and As_2 species from the surface during the growth of germanium films on Si(100) with continuous As_4 deposition is monitored using laser ionization time-of-flight mass spectrometry. A significant increase in the flux of As_2 from the surface is observed when the Ge flux is admitted to the surface. Upon discontinuation of the germanium growth process, the As_4 and As_2 signal levels remain at this increased level. A comprehensive study of the desorption fluxes of As_4, As_2, and As species from both Ge(100) and Si(100) substrates was performed as a function of substrate temperature and incident As_4 flux to determine the kinetics of desorption of the different species from the substrates. The behavior of the As_2 desorbed fluxes as a function of surface temperature is qualitatively different on the Ge(100) and Si(100) substrates. The results indicate that the catalytic cracking of As_4 to As_2 is more effective on Ge(100) compared to Si(100) at substrate temperatures between 800 and 1000 K, most likely because of more rapid desorption of As_2 at a given temperature on Ge(100). A phenomenological activation energy for the desorption of As atoms from Ge(100) of 1.2 ± 0.4 eV is also obtained. The implications for the surfactant enhanced growth of Ge on Si(100) are discussed.

Introduction

The growth of germanium thin films on silicon substrates has attracted a great deal of attention due to the many possible advantages that germanium and silicon/germanium films have for generating useful semiconductor nanostructures and optoelectronic devices.[1−4] However, the growth of germanium on a silicon surface does not in general result in a flat, uniform film. Germanium on Si(100) grows in the Stranski-Krastanov growth mode in which layer-by-layer growth for a few layers is followed by the onset of islanding. The critical thickness for the islanding transition in this system is 3−5 monolayers (ML), driven by the strain that builds up in the lattice due to the 4.2% lattice mismatch between silicon and germanium. This natural tendency to form islands has been exploited in this system[3−10] as well as in III−V and II−VI semiconductor systems[11−14] as a way to form self-assembled quantum dot structures.

The growth of flat germanium films on Si(100) has been accomplished by using the technique of surfactant enhanced epitaxy.[3,4] In this process, when the silicon surface is precoated with a layer of arsenic (or Sb or H) the transition from layer-by-layer growth to islanding is suppressed and relatively thick layers (>15 ML) of epitaxial germanium can be grown on the silicon surface. During growth, the arsenic layer "floats" to the surface as it exchanges with the incoming germanium atoms. There are a number of different proposals for the mechanism by which the exchange process takes place;[3,4,15−20] however, it has not been determined which of these mechanisms is operable. The arsenic floats to the surface because it is energetically more favorable to cap the dangling bonds on both the Si(100) and Ge(100) surfaces than to be buried at the interface. Theoretical estimates suggest that the difference in energy between the As/Ge/Si and Ge/As/Si arrangements is 1.7 eV per dimer.[4] The effectiveness of this growth process depends critically upon the kinetics of the arsenic/germanium exchange process and will be very sensitive to the growth parameters such as incident flux, surface temperature, and coverage. To control this growth process to yield the desired results, the details of the kinetics of arsenic interactions with these surfaces as well as the exchange process itself must be understood.

While the structures of arsenic-terminated silicon surfaces[21−29] are well understood, the kinetics of arsenic interactions with these surfaces have received relatively little attention.[30] It is known that arsenic forms dimer rows on both Si(100) and Ge(100) surfaces, leaving an arsenic passivated surface at 1 ML coverge with no reactive dangling bonds.[21] These arsenic terminated surfaces are much lower in energy than the Si(100) or Ge(100) surfaces because of this elimination of the dangling bonds.

The goal of the work presented here is to investigate in detail arsenic interactions with the Si(100) and Ge(100) surfaces and the behavior of the continuous flux of arsenic species during the growth of germanium thin films on Si(100). In all the experiments the incident flux is the As_4 species, on Si(100), with and without incident Ge, and on Ge(100). The kinetics of As_4, As_2, and As atoms desorbing or scattering from Ge(100) and Si(100) surfaces are studied and these results are compared with the results during the growth experiments of Ge on Si(100), which show changes in the desorbing fluxes of As_2 and As_4 during the germanium film growth. A phenomenological activation energy for the desorption of As atoms is also determined. To our knowledge this is the first report of the desorbing gas-phase species during the surfactant enhanced growth process. The differences between As_2 desorption from Si(100) observed previously[30] and that from Ge(100) are discussed.

* Corresponding Author. Fax: 1 303 492 5504. E-mail srl@jila.colorado.edu.

† Present Address: Department of Chemistry, University of Kansas, Lawrence KS 66045.

‡ Staff member, Quantum Physics Division, National Institute of Standards and Technology.

10.1021/jp012411n CCC: $22.00
Published on Web 05/29/2002

Experimental Section

The desorption or scattering of As_n species from Ge/Si(100) surfaces during the surfactant enhanced epitaxy of Ge on Si(100), as well as desorption of As_n species from Ge(100) and Si(100) surfaces, both under a continuous flux of As_4, is studied using single-photon time-of-flight mass spectrometry. These experiments are conducted in a home-built ultrahigh vacuum (UHV) chamber described in detail previously.[31] This chamber, with a base pressure of $\sim 5 \times 10^{-11}$ Torr ($\sim 7 \times 10^{-9}$ Pa), is equipped with Auger electron spectroscopy (AES) to probe the chemical composition of the surface, an Ar^+ sputter gun for surface cleaning, a quadrupole mass spectrometer, reflection high energy electron diffraction (RHEED) to determine surface structure, and a single-photon ionization time-of-flight mass spectrometer (SPI-TOFMS) to probe the gas-phase species above the sample, either in the incident beam or the scattered or desorbed products.

Two different types of experiments are described in this paper. In the first, the desorption of As_n species from a growing Ge film on a Si(100) substrate is monitored at a specific substrate temperature. In the second, the desorption of As_n species from Ge(100) and Si(100) is investigated as a function of surface temperature. Single photon ionization mass spectrometry is used to detect the scattered fluxes of As_4, As_2, and As atoms in both experiments. The photons used for the ionization are the 9th harmonic of a pulsed Nd:YAG laser (10.5 eV). The 9th harmonic is generated by tripling 355 nm light ($\sim$35 mJ/pulse at 100 Hz, 5 ns duration, generated by tripling the 1064 nm light in standard nonlinear crystals) in a static gas cell containing approximately 5 Torr of xenon. The 355 nm light is focused into the gas cell using a quartz lens, and the resulting 118 nm photons (from the four wave mixing process) are collimated using a LiF lens and enter the UHV chamber through a LiF window.[31] The conversion efficiency of this process is estimated to be 1×10^{-5}.[32,33] The 118 nm photons enter the chamber and propagate parallel to the substrate and intersect the gaseous species about 1 cm in front of the growing wafer. The electron beam propagates antiparallel to the laser beam and the diffraction pattern is viewed on a phosphor screen on the side of the chamber near where the laser beam enters. The geometry allows the SPI-TOFMS and RHEED measurements to be carried out simultaneously during growth without interfering with the incident molecular beams.

The Si(100) and Ge(100) surfaces are prepared by annealing in a vacuum to 1100−1300 K (higher temperatures for Si(100)) for approximately 2 min and then slowly cooling the sample to the desired temperature. In some cases the samples are also lightly sputtered with an Ar^+ beam (500−1000 eV, 3 min). Auger electron spectroscopy measurements show that this procedure produces a surface that is free of carbon and oxygen (within the $\sim$1% sensitivity limit of the instrument). Immediately after the surface is prepared, one of the two types of experiments is performed.

The As_4 beam used in these experiments is an effusive beam generated by heating elemental arsenic in a Knudsen cell. This cell also contains a cracker stage that can be used to dissociate the As_4 to form As_2, but this stage was not heated enough to crack the As_4 in these experiments, so the incident beam was a pure As_4 beam (checked using SPI-TOFMS). Therefore, any signal at the As_2 or As atom masses is generated by catalytic cracking of the As_4 by the surface. In these experiments, the laser has been positioned to detect primarily scattered As_n species. This is possible since the As oven is positioned at an angle of 22° below the surface normal, so positioning the laser high on the sample intersects only the scattered species.

Mass spectra are collected using a digital oscilloscope and signals at the relevant masses can be selected using boxcar integrators and monitored as a function of time during the growth run. The signals recorded in this way are proportional to the number density of molecules in the interaction region, but what is required is the relative flux of the different species. The signals are converted to values proportional to the fluxes by multiplying by a velocity correction factor $(T/M)^{1/2}$, where T is the substrate temperature and M is the mass of the species of interest. This assumes that the desorbing species have been thermally accommodated, have a velocity distribution that is characterized by the substrate temperature, and have similar angular distributions. This is not strictly true, but should be a reasonable approximation.

The sample is radiatively heated by a tungsten filament located a few millimeters behind the sample. In this way, the sample temperature can be varied from room temperature to about 1300 K (monitored by optical and IR pyrometry).

Results

In the first set of experiments, the desorption of arsenic species from the surface is monitored during the initial stage of surfactant enhanced epitaxial growth of Ge on Si(100). A clean, well-ordered Si(100) substrate is prepared as described above (confirmed by AES and RHEED measurements). The germanium and arsenic ovens are heated to give a flux of $\sim$1−10 ML/min of Ge and 1−8 ML/s of arsenic atoms. The arsenic oven is opened and mass spectra of the arsenic species desorbing from the surface are recorded.

At substrate temperatures above 600 K, the coverage of As on the surface saturates at 1 ML, therefore the majority of the incident As_4 beam is scattered directly from the surface. At temperatures below about 700 K, the only signal observed in the mass spectra is that of As_4. As the surface temperature is raised, As_2 begins to appear in the mass spectra. As the temperature is raised further, arsenic atoms also begin to desorb from the surface. The upper trace in Figure 1 shows a mass spectrum taken at 900 K of a Si(100) surface under a continuous flux of As_4. The large peak at mass 300 is due to As_4 scattered directly from the surface, and the signal at mass 150 is due to As_2 formed by dissociation at the surface.

The bottom trace in Figure 1 shows a mass spectrum taken immediately after the Ge shutter is opened. The same mass peaks are observed in this spectrum, but the intensities are dramatically changed. There is a significant decrease in the signal at the As_4 mass and a large increase at the As_2 mass. This shows that the process of depositing Ge on the Si(100) surface increases the desorption rate or probability of forming As_2. This can be seen as well in Figure 2 where the As_4 and As_2 mass signals are monitored as a function of time during the growth run. The arsenic oven is open throughout the run and the Ge shutter is opened at $t = 20$ s and closed again at $t = 40$ s. As the Ge shutter is opened, a decrease in As_4 signal and an increase in As_2 signal are observed, as in the previous mass spectra. However, when the germanium shutter is closed and growth is stopped, the signal levels remain constant. If the change in arsenic were due to dynamical exchange processes during growth, the signal levels would change again once the growth was terminated. This suggests that the kinetics of arsenic cracking and desorption from Ge surfaces and Si surfaces are different in some way.

To investigate the kinetics of As_n desorption from Ge(100) and Si(100), a second type of experiment was performed in

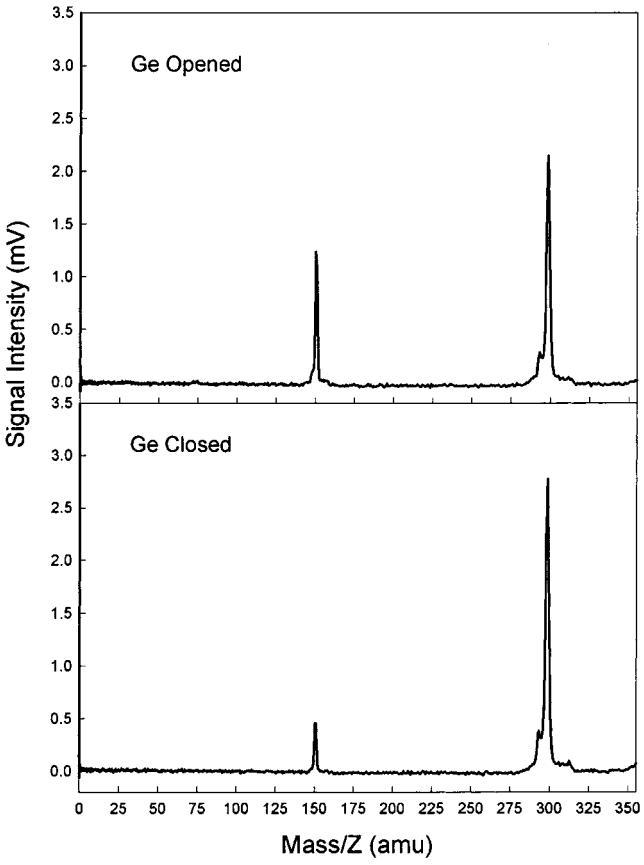

Figure 1. Mass spectra taken during the growth of Ge/Si(100) before growth begins (lower trace) and after the germanium shutter is open (upper trace). The peak at 300 amu is due to As_4 and the peak at 150 amu is due to As_2.

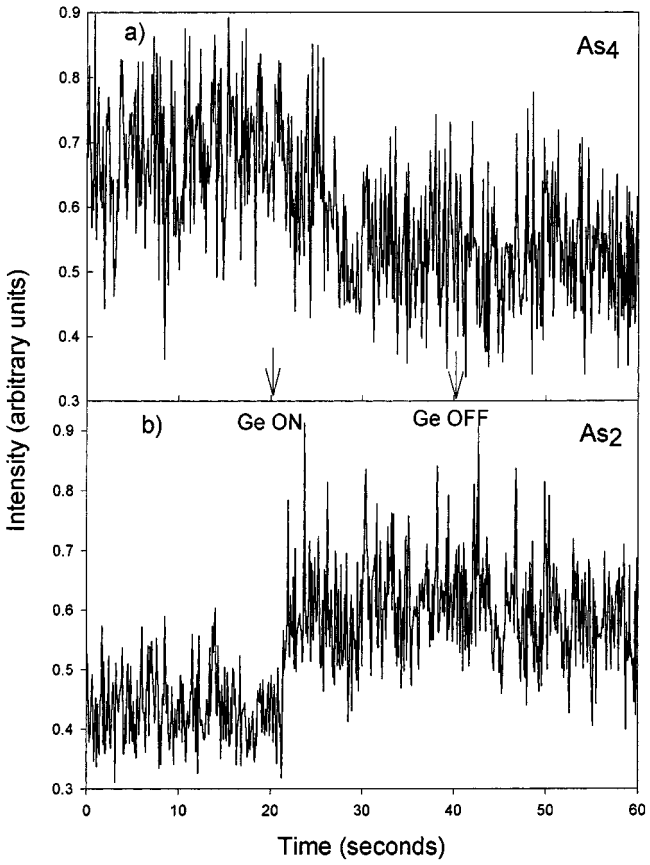

Figure 2. Real time measurement of mass signals during a growth run for As_4 (upper curve) and As_2 (lower curve). The arsenic oven was open during the entire experiment and the germanium oven was opened at $t = 20$ and closed at $t = 40$ s.

which the flux of As_4, As_2, and As atoms desorbing from both substrates was monitored as a function of surface temperature. The steady-state As_n signal levels are extracted from data where the sample is bathed in the As_4 for some time, then the As_4 shutter is closed and the background signal level in the chamber is recorded and subtracted from the signal with the shutter open. Figure 3 shows the results of an experiment of this type on a Ge(100) substrate with an incident As_4 flux of ~1 ML/s of arsenic atoms. The background signal due to the laser intersecting a small fraction of the incident As_4 beam has been subtracted out for all the figures. At low surface temperatures, the As_4 is simply scattered from the As-terminated Ge surface. As the surface temperature is raised, As_2 begins to evolve from the surface, with a simultaneous decrease in the As_4 signal. As stated above, as the arsenic dimers desorb from the surface, they open up reactive sites on the surface for As_4 to adsorb and react, therefore a decrease in the As_4 signal is observed. The relative sensitivities of As_4 and As_2 are approximately established by assuming that two arsenic dimers should be generated for each As_4 that is lost. The As_4 and As_2 data have been based on these sensitivity factors, but due to the low signal level for the As atom, the sensitivity has not been determined accurately and the raw fluxes are reported. These factors vary significantly depending on the settings of the electron multiplier (because of the high mass, the arsenic species are not detected efficiently), the deflectors, and einzel lens as well as the position of the laser beam within the extraction region of the time-of-flight. The results are also sensitive to angular factors, which are assumed to be similar. As the surface temperature is increased further, the As_4 and As_2 signals begin to plateau and a small signal is observed due to the desorption of arsenic atoms. This

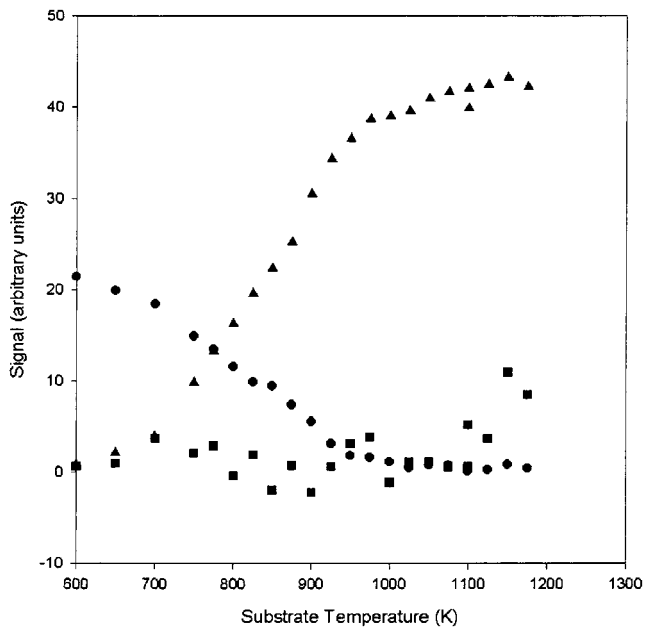

Figure 3. As_4 (circles), As_2 (triangles), and As atom (squares) desorption from Ge(100) with an incident As_4 flux of ~1 ML/s As atoms as a function of surface temperature.

is due to the dissociation of arsenic dimers on the surface at elevated temperatures. The error bars on the data in Figures 3−5 are approximately the size of the symbols (1−1.5%). The data for Figure 5 show results for arsenic on silicon.

Figure 4 shows data from the same type of experiment as in Figure 3, As_4 on Ge; however these data are collected at a

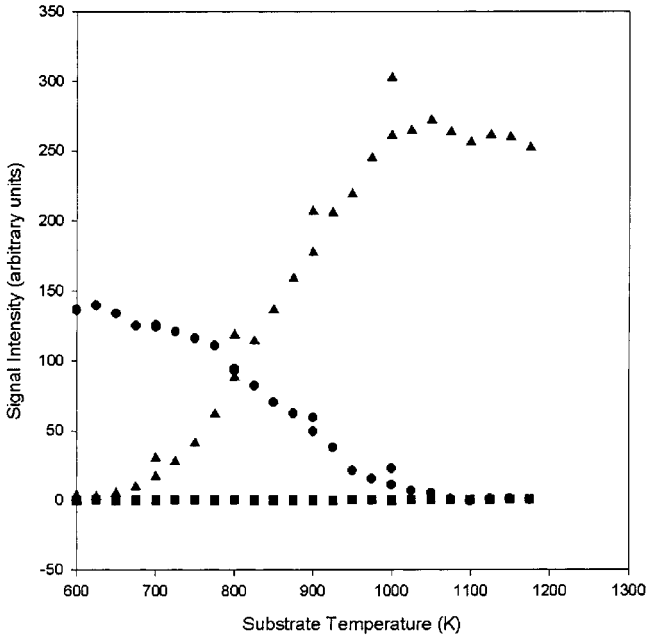

Figure 4. As_4 (circles), As_2 (triangles), and As atom (squares) desorption from Ge(100) with an incident As_4 flux of ~8 ML/s As atoms as a function of surface temperature.

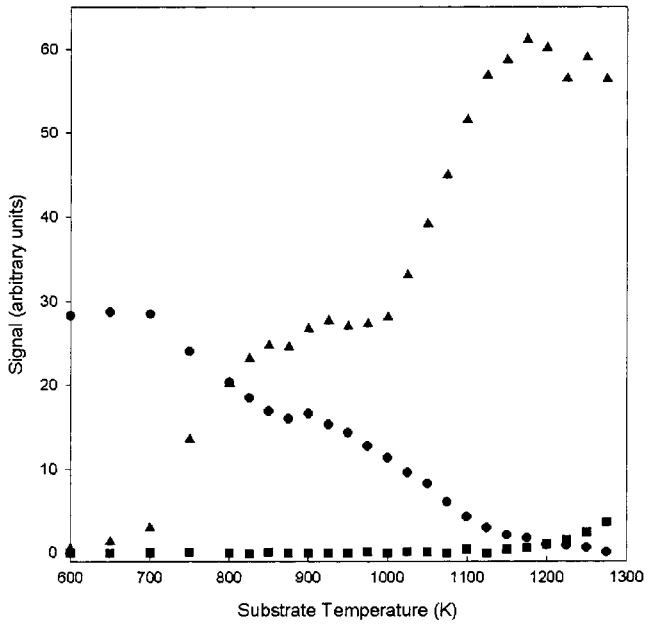

Figure 5. As_4 (circles), As_2 (triangles), and As atom (squares) desorption from Si(100) with an incident As_4 flux of ~2 ML/s As atoms as a function of surface temperature.

significantly higher incident As_4 flux. In this case, the arsenic flux is on the order of 8 ML/s. The overall shape of the desorption curves is identical to those at the lower flux, suggesting that the processes observed are not limited by the incident arsenic flux. Thus there is no site blocking and the rates of catalytic cracking are not limited by available sites on the surface.

From the high-temperature data in experiments such as those presented in Figures 3 and 4, it is possible to extract a phenomenological activation energy for the desorption of arsenic atoms from the Ge(100) surface. By plotting the logarithm of the arsenic atom signal as a function of $1/T$ (an Arrhenius plot), an activation energy of 1.2 ± 0.4 eV is extracted by averaging the results of three similar desorption runs. The Arrhenius plot

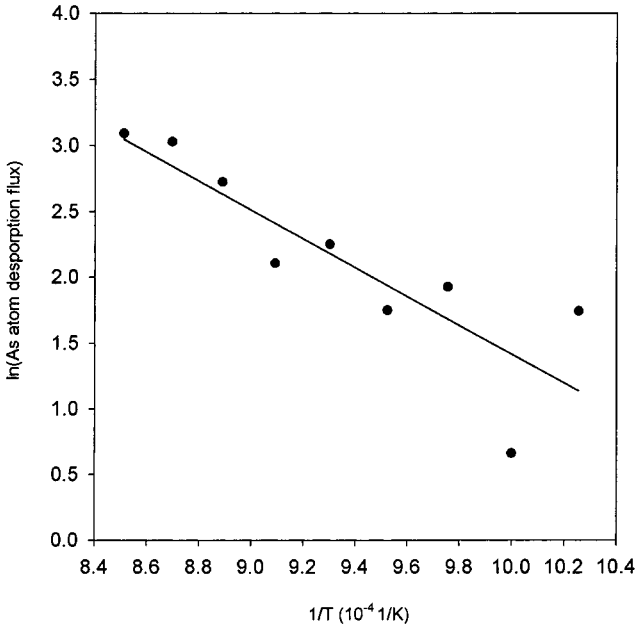

Figure 6. Data from Figure 4 shown as an Arrhenius plot. The slope of the best fit line is used to determine the activation energy.

obtained from the data in Figure 4 is shown in Figure 6. Note that even at the low signal levels in this experiment, a reasonable estimate of the slope and therefore the activation energy can be obtained. Unfortunately, the coverage of As_n species on the surface most likely changes significantly as a function of surface temperature, but we have no method to quantify this change in the present experiments under steady-state As_4 flux. The activation energy may be coverage dependent, and this will cause an error in the estimation of the activation energy by this method. In experiments at different incident arsenic fluxes, the activation energy did seem to decrease with increasing incident arsenic flux, but because of the low signal levels, this trend is not significant when compared with the error associated with the measurement.

In previous experiments, a phenomenological activation energy for arsenic atom desorption from Si(100) was determined to be 1.64 eV,[30] slightly higher than that determined here for Ge(100). This is not surprising since we anticipate from periodic properties that the As−Si bonds are stronger than the As−Ge bonds. However, it must be noted that these are phenomenological activation energies, possibly resulting from a complicated surface process involving diffusion to defects in addition to simple As−Ge or As−Si bond rupture, which we would expect to have much larger activation energies on the Si(100) or Ge(100) terraces. The exact nature of the process resulting in this phenomenological activation energy cannot be determined from these measurements, but it is clear that this must be something besides simple bond rupture.

Similar experiments have also been performed on a Si(100) surface. These experiments confirm the results of previous experiments in our group on the As/Si(100) system.[30] Figure 5 shows the results of such an experiment with an incident arsenic flux of ~2 ML/s of As atoms. Again, at very low surface temperatures, the only signal observed is As_4 and as the surface temperature is raised, As_2 begins to desorb from the surface as in the case of Ge(100). Also at very high temperatures, a signal due to As atoms desorbing from the surface is observed. In previous experiments, an activation energy for arsenic atom desorption from Si(100) was determined to be 1.64 ± 0.05 eV and the results presented here are consistent with this value.[30]

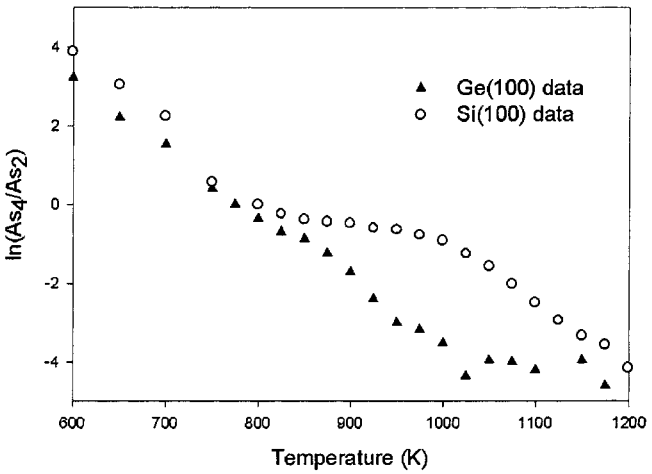

Figure 7. The natural logarithm of the ratio of the As_4 to As_2 signal is shown as a function of temperature. (The open circles are the Si(100) data and the filled triangles are the Ge(100) data). Note that the behavior is clearly different for these two substrates in the 800−1000 K range.

The plateau observed between 800 and 1000 K is always present in the case of Si(100) at all incident arsenic fluxes and laser probe positions that have been tried. In contrast, such a plateau is never observed in the case of Ge(100). To further illustrate this point, Figure 7 shows the $\ln(As_4/As_2)$ as a function of temperature for both the Si(100) and Ge(100) surfaces. In this plateau region, the Si(100) and Ge(100) surfaces behave very differently. This points to a fundamental difference in the arsenic desorption kinetics from Ge(100) and Si(100) surfaces.

Discussion

The structures of the arsenic terminated Si(100) and Ge(100) surfaces consist of rows of As dimers capping the dangling bonds of the Si (Ge) atoms underneath. At temperatures above ~600 K, the coverage of As saturates on the Si(Ge) surface at 1 ML. This has been observed in previous work and confirmed in these experiments by Auger electron spectroscopy measurements of the relative intensities of the Si(Ge) signals and the arsenic signal as a function of exposure time. At temperatures near 600 K, then, it is not surprising that the incident arsenic tetramers simply scatter from the arsenic terminated surface. As the surface temperature is raised, however, arsenic species desorb from both surfaces, opening up reactive sites for the adsorption and catalytic cracking of incoming As_4. This leads to the observed decrease in the As_4 signal as a function of surface temperature. At very high temperatures, the As_2 on the surface can dissociate and desorb as arsenic atoms. A series of reactions that is consistent with the observed data is

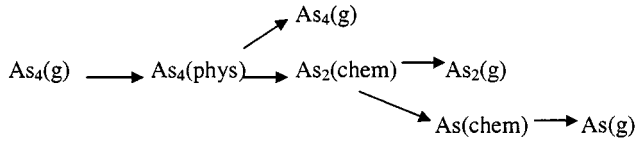

where (g) represents gas-phase species, (phys) means physisorbed, and (chem) means chemisorbed. The chemical balance is not shown.

The difference in the arsenic dimer signals as a function of temperature between the Si(100) surfaces and Ge(100) surfaces warrants discussion. The desorption of As_2 from these two surfaces is qualitatively different, with the Si(100) surface exhibiting a plateau between 800 and 1000 K and the Ge monotonically increasing over this temperature range. Several possibilities for the differences between these two surfaces are considered. First, the coverage of arsenic species on the surface may be different for Si and Ge at the same temperature, giving rise to differences in the desorption rates. We have no way to quantify this in the present experiment. In the previous experiments on Si(100) it was suggested that above 1050 K the steady-state coverage of As species on the terraces is quite small.[30] The temperature at which this occurs on Ge(100) could be significantly different. Second, there may be additional pathways for adsorption available for Si(100) compared to Ge(100) due to differences in the binding energetics. Finally, there is the possibility of a structural rearrangement of the steps on either the Si(100) or Ge(100) surface that would cause differences in the desorption of As_2. Both surfaces show 2×1 reconstructions in this temperature range, but the possibility of changing terrace widths or the formation of double-height steps on one surface or the other cannot be ruled out. Clearly, more detailed investigations of the steady-state structure and coverage of As species on these surfaces would aid in determining which of these possibilities is the most likely source of the difference in desorption rates.

In the growth experiments, where the fluxes of arsenic species desorbing from the surface during a growth run are measured, an increase in the As_2 signal and a corresponding decrease in the As_4 signal are observed. This is consistent with the results of the kinetics experiments that suggest qualitative differences in the desorption of As_2 on Si and Ge surfaces. As Ge is deposited, an arsenic terminated Ge surface is generated and the As_2 species observed are the result of interaction with this Ge covered surface instead of the original silicon surface. The fact that the signal levels do not change upon termination of the growth, even after several minutes, indicates that the differences are not due to Ge/As exchange processes occurring during growth.

The arsenic surfactant mediated growth of germanium on Si(100) relies on the arsenic remaining on the surface during the growth and not desorbing or being incorporated into the growing film. At growth temperatures used here (which are typical MBE growth temperatures) As_2 desorbs more readily from a germanium covered surface than from the original silicon surface. This may have an impact on the quality of Ge films generated, as the As may be lost during the growth process and the growth mode may change. This will be even more important in cases where a constant arsenic supply is not provided during the growth process. By making detailed measurements of this type, the complex processes controlling the surfactant mediated growth can be elucidated in more detail and the mechanism responsible for the change in growth mode from islanding to layer-by-layer growth can be determined.

Conclusions

The arsenic surfactant enhanced growth of germanium thin films on Si(100) has been studied using SPI-TOFMS to monitor the flux of As_n species desorbing from the surface into the gas phase during a growth run. The flux of As_2 from the surface increases when the germanium oven is opened while the flux of As_4 shows a corresponding decrease. This change is due to the difference in the kinetics of As_2 interaction with the original Si(100) surface and the germanium covered surface, which results after growth is started. The kinetics of As_4, As_2, and As atoms desorbing from both Ge(100) and Si(100) were measured by monitoring the desorbing fluxes as a function of surface temperature. The phenomenological activation energy for arsenic atoms desorbing from the Ge(100) surface was determined to

be 1.2 ± 0.4 eV, slightly less than that for As atoms desorbing from Si(100) determined previously (1.64 eV).[30]

Acknowledgment. Support for this work by DARPA and NSF is gratefully acknowledged. The authors also thank Sean Casey and Adina Ott for many useful discussions.

References and Notes

(1) Fujita, K.; Fukatsu, S.; Yaguchi, H.; Igarashi, T.; Shiraski, Y.; Ito, R. *Jpn. J. Appl. Phys.* **1990**, *29*, L1981.
(2) Osten, H. J.; Klatt, J.; Lippert, G.; Bugiel, E.; Higuchi, S. *J. Appl. Phys.* **1993**, *74*, 2507.
(3) Copel, M.; Reuter, M. C.; Kaxiras, E.; Tromp, R. M. *Phys. Rev. Lett.* **1989**, *63*, 632.
(4) Tromp, R. M.; Reuter, M. C. *Phys. Rev. Lett.* **1992**, *68*, 954.
(5) Seifert, W.; Carlsson, N.; Miller, M.; Pistol, M.-E.; Samuelson, L.; Wallenberg, L. R. *Prog. Crystal Growth Characterization* **1996**, *33*, 423.
(6) Wöhl, G.; Schöllhorn, C.; Schmidt, O. G.; Brunner, K.; Eberl, K.; Kienzle, O.; Ernst, F. *Thin Solid Films* **1998**, *321*, 86.
(7) Williams, R. S.; Medeiros-Ribeiro, G.; Kamins, T. I.; Ohlberg, D. A. A. *J. Phys. Chem.* **1998**, *102*, 9605.
(8) Williams, R. S.; Medeiros-Ribeiro, G.; Kamins, T. I.; Ohlberg, D. A. A. *Acc. Chem. Res.* **1999**, *32*, 425.
(9) Kamins, T. I.; Williams, R. S. *Appl. Phys. Lett.* **1997**, *71*, 1201.
(10) Chaparro, S. A.; Zhang, Y.; Drucker, J.; Chandrasekhar, D.; Smith, D. J. *J. Appl. Phys.* **2000**, *87*, 2245.
(11) Damilano, B.; Grandjean, N.; Massies, J.; Semond, F. *Appl. Surf. Sci.* **2000**, *164*, 241.
(12) Ishikawa, H.; Shoji, H.; Nakata, Y.; Mukai, K.; Sugawara, M.; Egawa, M.; Otsuka, N.; Sugiyama, Y.; Futatsugi, T.; Yokoyama, N. *J. Vac. Sci. Technol. A* **1997**, *16*, 794.
(13) Mukhametzhanov, I.; Heitz, R.; Zeng, J.; Chen, P.; Madhukar, A. *Appl. Phys. Lett.* **1998**, *73*, 1841.
(14) Pan, D.; Xu, J.; Towe, E.; Xu, Q.; Hsu, J. W. *Appl. Phys. Lett.* **1998**, *73*, 2164.
(15) Yu, B. D.; Oshiyama, A. *Phys. Rev. Lett.* **1994**, *72*, 3190.
(16) Boshart, M. A.; Bailes, A. A., III; Seiberling, L. E. *Phys. Rev. Lett.* **1996**, *77*, 1087.
(17) Kahng, S.-J.; Ha, Y. H.; Park, J.-Y.; Kim, s.; Moon, D. W.; Kuk, Y. *Phys. Rev. Lett.* **1998**, *80*, 4931.
(18) Ko, Y.-J.; Yi, J.-Y.; Park, S.-J.; Lee, E.-H.; Chang, K. J. *Phys. Rev. Lett.* **1996**, *76*, 3160.
(19) Ohno, T. *Phys. Rev. Lett.* **1994**, *73*, 460.
(20) Hwang, I.; Chang, T.; Tsong, T. T. *Phys. Rev. Lett.* **1998**, *80*, 4229.
(21) Bringans, R. D. *Crit. Rev. Solid State Mater. Sci.* **1992**, *17*, 353.
(22) Niehus, H.; Man, K.; Eldridge, B. N.; Yu, M. L. *J. Vac. Sci. Technol. A* **1988**, *6*, 635.
(23) Jedrecy, N.; Sauvage-Simkin, M.; Pinchaux, R.; Massies, J.; Greiser, N.; Etgens, V. H. *Surf. Sci.* **1990**, *230*, 197.
(24) Zegenhagen, J.; Patel, J. R.; Kincaid, B. M.; Golovchenko, J. A.; Mock, J. B.; Freeland, P. E.; Malik, R. J.; Huang, K.-G. *Appl. Phys. Lett.* **1988**, *53*, 252.
(25) Becker, R. S.; Klistner, T.; Vickers, J. S. *J. Microsc.* **1988**, *152*, 157.
(26) Bringans, R. D.; Olmstead, M. A.; Uhrberg, R. I. G.; Bachrach, R. Z. *Appl. Phys. Lett.* **1987**, *51*, 523.
(27) Bringans, R. D.; Olmstead, M. A.; Uhrberg, R. I. G.; Bachrach, R. Z. *Phys. Rev. B* **1987**, *36*, 9569.
(28) Bringans, R. D.; Biegelsen, D. K.; Swartz, L.-E. *Phys. Rev. B* **1991**, *44*, 3054.
(29) Uhrberg, R. I. G.; Bringans, R. D.; Bachrach, R. Z.; Northrup, J. E. *Phys. Rev. Lett.* **1986**, *56*, 520.
(30) Ott, A. K.; Casey, S. M.; Leone, S. R. *Surf. Sci.* **1998**, *405*, 228.
(31) Ott, A. K.; Casey, S. M.; Alstrin, A. L.; Leone, S. R. *J. Vac. Sci. Technol. B* **1996**, *14*, 2742.
(32) Hilbig, R.; Wallenstein, R. *IEEE J. Quantum Electron.* **1981**, *17*, 1566.
(33) Pallix, J. B.; Schule, U.; Becker, C. H.; Huestis, D. L. *Anal. Chem.* **1989**, *61*, 805.